



Bioelectricity inhibits back diffusion from the anolyte into the desalinated stream in microbial desalination cells



Qingyun Ping^a, Oded Porat^b, Carlos G. Dosoretz^{b, **}, Zhen He^{a, *}

^a Department of Civil and Environmental Engineering, Virginia Polytechnic Institute and State University, Blacksburg, VA 24061, USA

^b Faculty of Civil and Environmental Engineering, Technion-Israel Institute of Technology, Haifa 32000, Israel

ARTICLE INFO

Article history:

Received 30 July 2015

Received in revised form

12 October 2015

Accepted 13 October 2015

Available online 22 October 2015

Keywords:

Microbial desalination cells

Back diffusion

Wastewater treatment

Donnan effect

Molecular transport

ABSTRACT

Microbial desalination cells (MDCs) taking advantage of energy in wastewater to drive desalination represent a promising approach for energy-efficient desalination, but concerns arise whether contaminants in wastewater could enter the desalinated stream across ion exchange membranes. Such back diffusion of contaminants from the anolyte into the desalinated stream could be controlled by two mechanisms, Donnan effect and molecule transport. This study attempted to understand those mechanisms for inorganic and organic compounds in MDCs through two independently conducted experiments. Donnan effect was found to be the dominant mechanism under the condition without current generation. Under open circuit condition, the MDC fed with 5 g L⁻¹ salt solution exhibited 1.9 ± 0.7%, 10.3 ± 1.3%, and 1.8 ± 1.2% back diffusion of acetic, phosphate, and sulfate ions, respectively. Current generation effectively suppressed Donnan effect from 68.2% to 7.2%, and then molecule transport became more responsible for back diffusion. A higher initial salt concentration (35 g L⁻¹) and a shorter HRT (1.0 d) led to the highest concentration gradient, resulting in the most back diffusion of 7.1 ± 1.2% and 6.8 ± 3.1% of phosphate and sulfate ions, respectively. Three representative organic compounds were selected for test, and it was found that organic back diffusion was intensified with a higher salt concentration gradient and molecular weight played an important role in compound movement. Principal component analysis confirmed the negative correlation between Donnan effect and current, and the positive correlation between molecule transport and concentration gradient related conditions.

© 2015 Elsevier Ltd. All rights reserved.

1. Introduction

Microbial desalination cell (MDC) is a promising bio-electrochemical system for water supply with simultaneous wastewater treatment and saline water desalination. With anion exchange membrane (AEM) and cation exchange membrane (CEM) installed between the anode and the cathode, an MDC takes advantage of the electrical field generated by anode microbial metabolism and cathode (oxygen) reduction reaction to separate ions in salt solution between the two ion-exchange membranes (Cao et al., 2009). The mechanism of ion separation in an MDC is similar to that of electrodialysis (ED), but its driving force is the energy extracted from organic matters in wastewater by microorganism in the anode. Therefore, an MDC does not require external

electrical energy but generates electricity during desalination. As a result, energy consumption by desalination can potentially be low, compared with ED or other industrialized desalination technologies.

MDCs have been developed in two major configurations, cubic shape (Mehanna et al., 2010; Ping and He, 2013) and tubular shape (Jacobson et al., 2011a, 2011b). The desalination can be enhanced through stacked cells (Chen et al., 2011; Kim and Logan, 2011), electrolyte recirculation (Chen et al., 2012a; Qu et al., 2012), applying small external voltage (Ge et al., 2014), incorporating forward osmosis membrane in situ (Zhang and He, 2012) or ex situ (Yuan et al., 2015), adding ion exchange resin (Zhang et al., 2012), or integrating capacitive adsorption (Forrestal et al., 2012). Hydrogen and other chemicals can be produced by combining electrolysis with an MDC (Chen et al., 2012b; Luo et al., 2011). The scale of MDCs has been advanced from milliliters to over 100 L (Zhang and He, 2015). In addition to engineering development, MDCs have also been investigated with fundamental studies on multi-ion transport behavior from the salt solution (Luo et al., 2012a; Zuo et al., 2013),

* Corresponding author.

** Corresponding author.

E-mail addresses: carlosd@technion.ac.il (C.G. Dosoretz), zhenhe@vt.edu (Z. He).

inter-membrane distance (Ping and He, 2014), microbial community in MDC (Luo et al., 2012b), and mathematical modeling (Ping et al., 2014).

Having the adjacent anode compartment containing wastewater separated from salt solution by one piece of AEM, MDCs generate concerns of the crossover of organic and inorganic contaminants from wastewater into the desalinated stream. Our previous study of an MDC operated with a high acetate concentration discovered extensive back diffusion of acetic ions from the anolyte into the salt solution opposite the electrical field, thereby lowering the effluent quality and causing bio-fouling (Ping et al., 2013). We also observed that an MDC fed with wastewater ($\sim 260 \text{ mg L}^{-1}$ total organic carbon) exhibited mild organic back diffusion ($\sim 7 \text{ mg L}^{-1}$) in the desalinated effluent (Ping et al., 2015). It is reported that substances with negative or neutral charge and with molecular weight less than 350 Da can be transported through AEM (Kim and Logan, 2013). Most inorganic anions can freely cross AEM, and thus back diffusion of anions from the anolyte into the salt solution against the electrical field is expected to occur to some degree. Industrialized AEMs usually do not have an ideal 100% permselectivity, and would allow co-ions (cations) to pass through (Strathmann, 2004). As a result, there is a great possibility that cationic contaminants may be found in the desalinated stream. MDCs are proposed as a pre-desalination process for seawater desalination, or desalinating brackish water; in either application, back diffusion of inorganic ions and organic substances could deteriorate the quality of the desalinated water and create requirement for additional treatment at an expense of cost and time. Therefore, understanding the process of back diffusion is of great importance for the development of MDC technology. So far there has not been any research focusing on the issue of back diffusion of contaminants in an MDC, which warrants our motivation of this study.

Herein, we proposed two mechanisms of back diffusion in an MDC: first, simple anion exchange (Donnan effect) through AEM with chloride ions in the salt solution moving towards the anolyte by a concentration gradient while forcing anion or negatively charged organics in the anolyte moving into the desalinated stream to balance the charge; and second, molecule transport of equally charged anion and cation or neutral charged organics from the anolyte into the desalinated stream through AEM. Water transport (driven by a concentration gradient) from the anolyte to the salt solution could promote molecule transport, and a high concentration of chloride ion in the salt solution will promote the Donnan effect. However, current generation would inhibit the Donnan effect. To understand above mechanisms and their effects on back diffusion, we have conducted the MDC experiments fed with synthetic wastewater by 1) manipulating the electric current, an opposing force of back diffusion, 2) altering the salt concentration gradient, a key factor for back diffusion, and 3) varying the salt solution retention time, which is related to salt solution–anolyte interaction time.

2. Materials and methods

2.1. MDC setup and operation

The study of inorganic back diffusion was conducted with an MDC that was assembled in a tubular shape similarly to the one in the previous study (Ping et al., 2014), which consisted of two layers of ion exchange membranes (IEM): the inner anion exchange membrane (AEM, AMI-7001, Membrane International, Inc., Glen Rock, NJ, USA) forming the anode compartment (300 mL, diameter of 3.8 cm) with a 20-cm long carbon fiber brush anode electrode inserted inside, and the outer cation exchange membrane (CEM,

diameter of 5 cm, CMI-7000, Membrane International, Inc.) wrapped by a piece of carbon cloth coated with activated carbon supported platinum (Pt/C) catalyst (loading rate of $0.2 \text{ mg Pt cm}^{-2}$) as the cathode electrode. The space between those membranes formed a desalination compartment (150 mL). The two ion exchange membrane tubes were sealed at both ends to PVC caps with robust epoxy glue. An external resistor was applied by connecting the two electrodes with titanium wire. The anode feed solution was a synthetic solution containing (per L of tap water): NaAc, 0.5 or 1 g; NH_4Cl , 0.15 g; NaCl, 0.5 g; MgSO_4 , 0.015 g; CaCl_2 , 0.02 g; KH_2PO_4 , 0.53 g; and K_2HPO_4 , 1.07 g. The phosphate concentration was higher than that of a typical domestic wastewater, because of the need for buffering the anolyte. The salt solution in the desalination compartment was prepared by dissolving NaCl in tap water. The catholyte was tap water (to ensure that the anolyte was the only source responsible for back diffusion), dripping from the top to the bottom of the outer (CEM) tube for rinsing the cathode electrode, and recirculated at a rate of 35 mL min^{-1} from a 9-L reservoir. The anolyte had a feeding rate of 0.5 mL min^{-1} , resulting in a hydraulic retention time (HRT) of 10 h, and was recirculated at 100 mL min^{-1} . The salt solution had a feeding rate of 0.06 or 0.1 mL min^{-1} that had HRT of 1.7 or 1.0 day.

The MDC for characterization of organic back diffusion was set up in a biotic or abiotic environment with an anode volume of 1000 mL and a desalination compartment volume of 250 mL. Three organics were tested, acetate, Paracetamol (PCM) and Ibuprofen (IBP). Acetate represents small, negatively charged and hydrophilic organic compounds in wastewater. PCM and IBP represent neutral and negatively charged micro-pollutants in municipal wastewater, respectively, of relatively low hydrophobicity. The anode feed solution contained (per L of tap water): (in biotic MDC) NaAc, 1000 mg; PCM, 10 mg; IBP, 10 mg; KH_2PO_4 , 2.6 g; K_2HPO_4 , 5.4 g; NH_4Cl , 0.04 g; NaCl, 0.45 g; MgSO_4 , 0.2 g; CaCl_2 , 0.015 g and NaHCO_3 , 2 g; and Sigma solution (Velasquez-Orta et al., 2010), 5 mL; or (in abiotic MDC) each representative organics, 100 mg; NaN_3 (biocide), 100 mg; KH_2PO_4 , 2.6 g and K_2HPO_4 , 5.4 g. The salt solution in the desalination compartment was prepared with 10 g L^{-1} NaCl in tap water in biotic MDC, or in abiotic MDC with: NaN_3 (biocide), 100 mg; KH_2PO_4 , 2.6 g; K_2HPO_4 , 5.4 g; with or without NaCl, 10 g. The cathode for biotic MDC was rinsed with solution from a 500 mL container containing (per L of tap water) KH_2PO_4 , 2.6 g and K_2HPO_4 , 5.4 g, at recirculation rate of 60 mL min^{-1} . The abiotic MDC was operated with a dry cathode to avoid complications. Both MDCs were operated in a batch mode and solution samples were collected after 2 d of retention time.

2.2. Measurement and calculations

The MDC voltage was recorded every 3 min using a digital multimeter (Keithley Instruments, Inc., Cleveland, OH, USA). The conductivity of the salt solution was measured using a benchtop conductivity meter (Mettler-Toledo, Columbus, OH, USA). The chemical oxygen demand (COD) was measured using a colorimeter according to the manufacture manual (Hach Company, Loveland, CO USA). The ion compositions in the solution were measured using ion chromatography (Dionex DX-500) with suppressed conductivity detection. The column used for cations was a CS-16 with a CSRS-300 suppressor and for anions was an AS-9HC with an ASRS-300 suppressor. The concentrations of pharmaceuticals were tracked by liquid chromatography-multiple stage/mass spectrometry (LCMS/MS) (Vanderford et al., 2003; Gur-Reznik et al., 2011). Injections were performed on an Agilent 1200 HPLC (Hewlett Packard) system coupled with an ion spray interface to an API 3200 triple quadrupole mass spectrometer (Applied Biosystems). A LiChroCART Purospher STAR RP-18 (Merck) end capped column

(4.6 mm × 15 cm, 5 μm pore size) was used with a binary gradient of 0.1% (v/v) formic acid in water and HPLC grade methanol. Electro spray ionization was used in positive ion mode for PCM, and in negative ion mode for IBP with the limit of quantification of 5 μg L⁻¹. The compounds were detected in multiple-reaction monitoring (MRM) mode. Acetate concentration was measured in an 881 compact IC Pro ion chromatograph (Metrohm), equipped with Metrohm A supp 5–150 (with 4 μm pore size) column, and the limit of quantification was 1 mg L⁻¹. A solution of 3.2 mM sodium carbonate and 1.0 mM sodium bicarbonate in 5% acetonitrile was used as eluent. The back diffusion percentage for each ion in continuous operated MDC was calculated by excluding tap water ion concentration as shown in equation (1). It is worth noting that current-driven ion migration and back diffusion are in opposite directions, and back-diffused ions can also be removed from the desalination compartment by current. These two processes are happening simultaneously. Here we quantified the back diffusion as the result of the two mixed effects, which are directly observable:

$$\text{Back diffusion \%} = \frac{(C_{\text{salt,out}} - C_{\text{tap}})Q_{\text{salt}}}{C_{\text{anode,in}}Q_{\text{anode}}} \quad (1)$$

where $C_{\text{salt,out}}$ is the ion concentration in the desalinated stream, C_{tap} is the ion concentration in the tap water, $C_{\text{anode,in}}$ is the ion concentration in the anolyte influent, Q_{salt} is the salt solution flow rate, and Q_{anode} is the anolyte flow rate.

The back diffusion percentage and adsorption percentage on the AEM for each organic compound in the batch mode MDC was calculated by Equations (2) and (3):

$$\text{Back diffusion \%} = \frac{C_{\text{salt,t}} V_{\text{salt,t}}}{C_{\text{anode,0}} V_{\text{anode,0}}} \quad (2)$$

$$\text{Adsorption \%} = \frac{(C_{\text{anode,0}} V_{\text{anode,0}} - (C_{\text{anode,t}} V_{\text{anode,t}} + C_{\text{salt,t}} V_{\text{salt,t}}))}{C_{\text{anode,0}} V_{\text{anode,0}}} \quad (3)$$

where $C_{\text{anode,0}}$ is the initial organic compound concentration in the anolyte, $C_{\text{salt,t}}$ and $C_{\text{anode,t}}$ are the organic compound concentrations at time t (2 d in this study) in the salt solution and anolyte, $V_{\text{anode,0}}$ is the initial volume of the solution in the anode compartment, $V_{\text{salt,t}}$ and $V_{\text{anode,t}}$ are the volumes of the solution in desalination and anode compartments at time t .

The percentage of back diffusion contributed by molecule transport and Donnan effect were calculated by Equations (4) and (5), respectively. The back-diffused cations are caused by molecule transport from the anolyte, while the back-diffused anions are a result of both molecule transport and Donnan effect:

$$\text{Molecule transport \%} = \frac{q_{\text{cation,total}}}{q_{\text{anion,total}}} \quad (4)$$

$$\text{Donnan effect \%} = \frac{(q_{\text{anion,total}} - q_{\text{cation,total}})}{q_{\text{anion,total}}} \quad (5)$$

where $q_{\text{cation, total}}$ is the total charge of contaminant cations in the desalinated stream, and $q_{\text{anion, total}}$ is the total charge of contaminant anions in the desalinated stream. Based on the pH value of the salt solution, the hydrolytic equilibrium of phosphate ion was applied in determining its form (hydrogen phosphate ion or dihydrogen phosphate ion), which affects the calculation of total charge of anions.

The osmotic water flux from the anolyte to the salt solution was calculated according to Van't Hoff's equation as in Equation (6):

$$Q_{\text{osmosis}} = A_{\text{AEM}}RTi(C_{\text{salt,out,total}} - C_{\text{anode,out,total}}) \quad (6)$$

where A_{AEM} is the water permeability of AEM, R is the gas constant, T is the temperature, i is the Van't Hoff factor, and the last part of the equation is the total mole concentration difference between the desalinated stream and anolyte effluent.

Principal component analysis (PCA) as a multivariate statistical tool was performed in R to determine the key factors causing back diffusion. The data matrix was scaled to have a mean of 0 and standard deviation of 1 to ensure equal weights of all variables before singular value decomposition was done. PCA transforms original variables into new uncorrelated variables called principal components. The first component (PC1) contains the highest variance, and the second component (PC2) has the second highest variance. Biplot displays the loadings (for the variables) and scores (for the samples) generated from PCA to visualize the similarity or difference between samples.

3. Results and discussion

3.1. Effect of current generation on inorganic back diffusion

Theoretically, current generation drives anion movement from the desalination compartment to the anode compartment, against back diffusion. The actual effect of current generation on back diffusion of inorganic ions was investigated by varying external resistance loading (which changed current generation) with an initial salt solution concentration of 5 or 35 g L⁻¹. By examining the anolyte composition, three anions (acetic, phosphate, and sulfate ions) and three cations (magnesium, potassium, and calcium ions) were selected as dominant back diffusion ionic species for study. Acetic ion is listed here because acetate was the substrate for microorganism growth, and contributed to total back diffusion. Sodium and chloride ions were excluded from back diffusion ions, because they were the native ions in the salt solution with significantly high concentrations. There is a clear trend that with the increased current the back diffusion of anions was suppressed under both initial salt concentrations (Fig. 1). At 0 current generation (open circuit-OC that does not have current-driven anion movement from the desalination compartment to the anolyte) with an initial salt of 5 g L⁻¹, the back diffusion percentages of acetic, phosphate, and sulfate ions were 1.9 ± 0.7%, 10.3 ± 1.3%, and 1.8 ± 1.2%, respectively. When an external resistor of 100 Ω was applied to increase the current generation to 13.0 A m⁻³ (desalination efficiency of 41.3 ± 1.9% with current-driven anion movement, mostly chloride ions, from the desalination compartment to the anolyte at a rate of 23.2 mmol L⁻¹ d⁻¹), the back diffusion percentages of those three anions decreased to 0.3 ± 0.1%, 4 ± 0.7%, and 0%, respectively. Further increasing current production to 26.7 A m⁻³ by reducing external resistance to 0.1 Ω (desalination efficiency of 79.2 ± 4.7% with current-driven anion movement at a rate of 47.8 mmol L⁻¹ d⁻¹) almost inhibited the crossover of acetic and sulfate ions completely, and reduced the back diffusion percentage of phosphate ions to 2.3 ± 0.4% (Fig. 1A). The experiment with 35 g L⁻¹ of the initial salt concentration showed the same trend for individual back diffusion due to current effect, with the back diffusion percentages of acetic, phosphate, and sulfate ions at 4.7 ± 0.2%, 17.5 ± 4.4%, and 11.8 ± 1.4% at zero current, which decreased to 2.0 ± 2.8%, 5.7 ± 1.9%, and 4.6 ± 4.3%, respectively, at current generation of 34.2 A m⁻³ (desalination efficiency of 49.0 ± 0.4% with current-driven anion movement at a rate of 61.2 mmol L⁻¹ d⁻¹) (Fig. 1B). There is no notable trend in the back

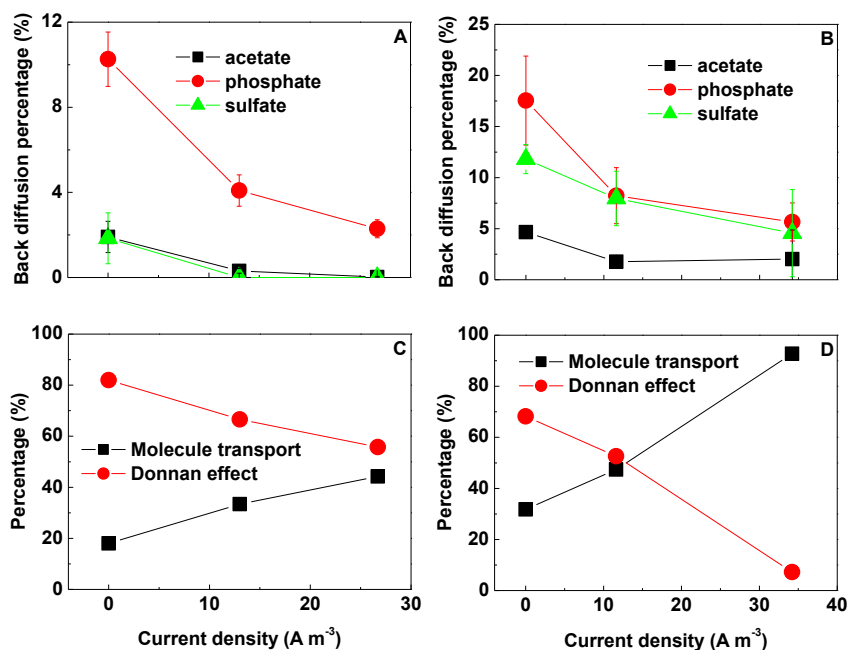


Fig. 1. Back diffusion of anions and contribution of each mechanism to back diffusion affected by current generation: (A) anion back diffusion at an initial salt concentration of 5 g L^{-1} ; (B) anion back diffusion at an initial salt concentration of 35 g L^{-1} ; (C) contribution of each mechanism to back diffusion at an initial salt concentration of 5 g L^{-1} ; and (D) contribution of each mechanism to back diffusion at an initial salt concentration of 35 g L^{-1} .

diffusion of cations under different current generation (Fig. 2); however, the data provide useful information in obtaining the molecule transport and Donnan effect percentage (Equations (4) and (5)).

The high salinity in the salt solution and low salinity in the anolyte creates a concentration gradient, which may play different

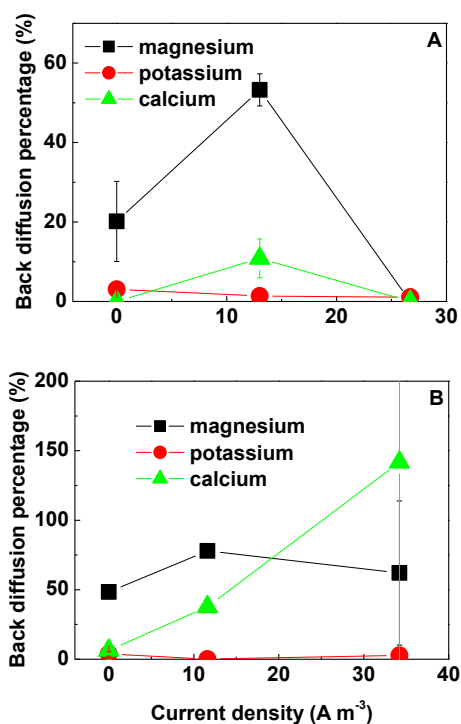


Fig. 2. Back diffusion percentage of different cations in MDC at different current generation with initial salt concentration of A) 5 g L^{-1} and B) 35 g L^{-1} .

roles in the two back-diffusion mechanisms. In the Donnan effect, the abundant chloride ions in the salt solution move through AEM to the anolyte due to the chloride concentration difference and this movement forces other anions in the anolyte to migrate into the salt solution. Because the concentration gradient is mainly caused by NaCl in the salt solution, the higher initial salt concentration would lead to a greater Donnan effect. In the molecule transport, a higher concentration gradient leads to a higher osmotic pressure and thus more water transport from the anolyte to the salt solution, which drives more molecules to transfer to the salt solution. Current generation results in a lower salinity in the salt solution, and decreases the concentration gradient between the anolyte and the salt solution. Therefore, current and concentration gradient have contradictory effects on back diffusion.

In the test with 5 g L^{-1} initial salt concentration, both higher current and resulted smaller concentration gradient between the salt solution and the anolyte (-1.9 mS cm^{-1} at 26.7 A m^{-3} compared with 1.2 mS cm^{-1} at 13.0 A m^{-3} , and 4.6 mS cm^{-1} at 0 A m^{-3}) led to less back diffusion. Having the same concentration gradient variation trend caused by current generation, the test with 35 g L^{-1} initial salt concentration had approximately two times the back diffusion percentage compared with 5 g L^{-1} at each current generation condition (Fig. 1A and B). The cause of more severe back diffusion was the higher concentration gradient which increased from -1.9 – 4.6 mS cm^{-1} with 5 g L^{-1} to 28.0 – 35.4 mS cm^{-1} with 35 g L^{-1} . The effect of different initial salt concentrations on back diffusion will be discussed in details in the next section.

The Donnan effect was more influential than the molecule transport at no current generation. The molecule transport accounted for 18.0% (or 31.8%) of the total back diffusion at 5 g L^{-1} (or 35 g L^{-1}), and Donnan effect accounted for 82.0% (or 68.2%) (Fig. 1C&D). Current generation suppressed the relative Donnan effect, and led to higher relative molecule transport. At 26.7 A m^{-3} , the two mechanisms accounted nearly 50% each for the back diffusion at 5 g L^{-1} initial salt concentration. Increasing the salt concentration to 35 g L^{-1} decreased the Donnan effect generally,

likely because of stronger molecule transport due to higher concentration gradient. The molecule transport accounted for 92.8% of the total back diffusion, and Donnan effect accounted for 7.2% at current generation of 34.2 A m^{-3} , indicating that Donnan effect was almost inhibited due to strong anion movement from the salt solution to the anolyte driven by current, and molecule transport was most responsible for the back diffusion (Fig. 1D).

3.2. Effect of initial salt concentration and salt retention time on inorganic back diffusion

The experiments were conducted at external resistance of 0.1Ω (for high current generation) under two sets of conditions, a flow rate of 0.06 or 0.1 mL min^{-1} (HRT of 1.7 and 1.0 d) and the initial salt concentration of 5 or 35 g L^{-1} . The desalination efficiency ranged from 25.4 to 79.2% , and a longer HRT or a lower initial salt concentration resulted in higher desalination efficiency.

A higher initial salt concentration promoted back diffusion. For example, the initial salt concentration of 35 g L^{-1} resulted in $4.2 \pm 2.0\%$ and $7.1 \pm 1.2\%$ of phosphate back diffusion at HRT 1.7 and 1.0 d , respectively, much higher than $2.3 \pm 0.4\%$ and $6.6 \pm 0.6\%$ with 5 g L^{-1} . Similar results were obtained with sulfate back diffusion that had $2.2 \pm 0.4\%$ and $6.8 \pm 3.1\%$ with 35 g L^{-1} under two HRTs, and there was no observable back diffusion with 5 g L^{-1} . Almost no acetate ions were found in the salt solution under these testing conditions (Fig. 3A), likely due to the high current generation at 26.7 – 28.2 A m^{-3} . Higher initial salt concentration also brought in more back diffusion of cations (magnesium and calcium) with 35 g L^{-1} , of which the greater than 100% back diffusion was due to the extreme small concentration of magnesium and calcium in the anolyte (less than 10 mg L^{-1}), and even a little residual in the desalination compartment or desorption from the ion exchange membranes could raise the percentage dramatically. There was no observable back diffusion of magnesium and calcium with 5 g L^{-1} .

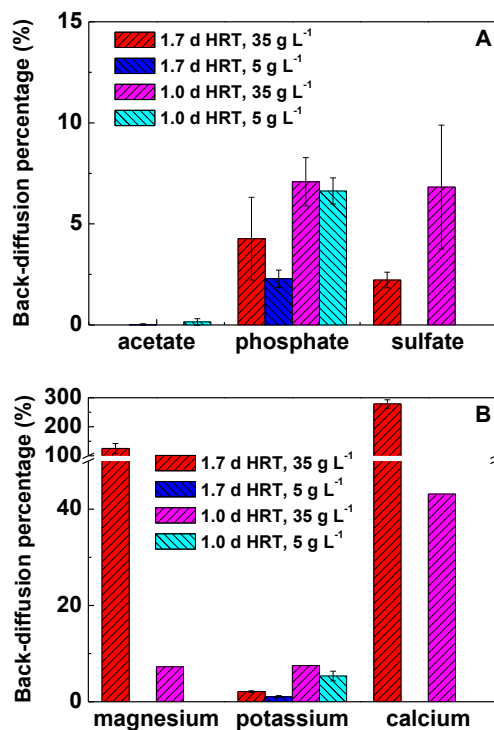


Fig. 3. Back diffusion affected by HRTs and initial salt concentrations: (A) anion back diffusion; (B) cation back diffusion.

The change of the back diffusion of potassium due to initial salt concentration was not distinct (Fig. 3B).

A higher salt concentration in the salt solution is expected to have a greater Donnan effect, considering that more chloride ions would exchange more anions in the anolyte. However, that was not supported by the experimental results shown in Fig. 4A, which exhibits stronger effect of molecule transport on back diffusion when the salt concentration gradient was high. Donnan effect was inhibited under high current generation, and the high salt concentration in the salt solution mainly contributed to molecule transport back diffusion. Molecule transport was severe at high salt initial concentrations, the greater concentration gradient between the anolyte and the salt solution (32.3 and 39.6 mS cm^{-1} at 35 g L^{-1} (Fig. 4B)) led to more water transport across the AEM towards the salt solution (0.009 and $0.010 \text{ mL min}^{-1}$ at 35 g L^{-1}), and as expected brought more back-diffused salts into the salt solution. The negative value of Donnan effect or the $>100\%$ molecule transport was due to the fact that back-diffused cations were more than anions, probably because back-diffused anions were removed out of the salt solution by current.

A shorter HRT accelerated the back diffusion due to a greater overall concentration gradient that enhanced both the Donnan effect and molecule transport. While the ratio of osmotic water flux

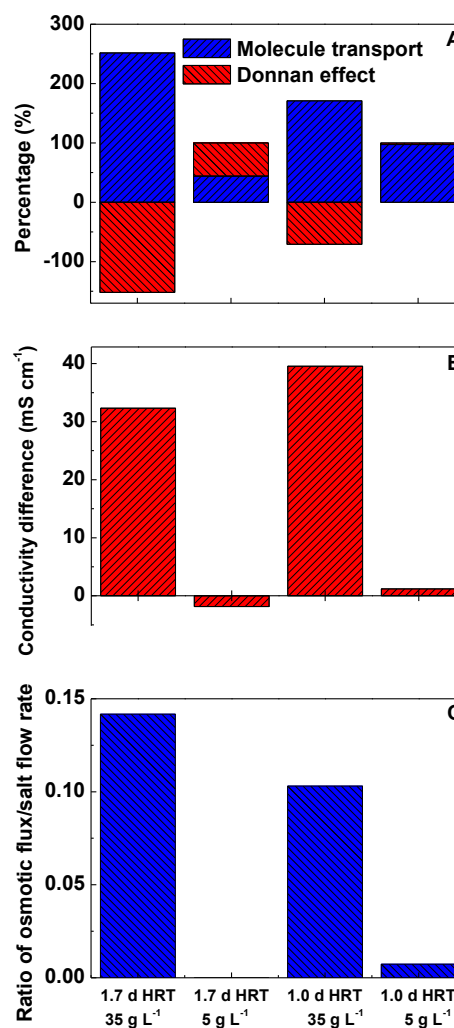


Fig. 4. Back diffusion affected by HRTs and initial salt concentrations: (A) contribution of Donnan effect and molecule transport attribution to back diffusion; (B) concentration gradient between the anolyte and the salt solution; and (C) the ratio between osmotic water flux and salt solution flow rate.

over salt solution flow rate that determined the severity of molecule transport was lower at longer HRT with 5 g L^{-1} , and higher at longer HRT with 35 g L^{-1} . With 5 g L^{-1} , the molecule transport effect was much greater (97.2%) than Donnan effect (2.8%) at HRT 1.0 d, while the two mechanisms had comparative effect at HRT 1.7 d. The ratio of osmotic water flux over salt solution flow rate indicated an insignificant amount of water was transported from the salt solution to the anolyte (opposite direction of osmotic water flux) at 1.7 d HRT, while at HRT 1.0 d water was transported from the anolyte to the salt solution at a flow rate ratio of 0.007 (Fig. 4C). When the osmotic water flux exhibited opposite direction, the molecule transport of other anions from the anolyte to the salt solution was only caused by the individual anion concentration differences between the anolyte and the salt solution, and thus molecule transport was not significant at 1.7 d HRT. The osmotic water flux was more significant with a higher initial salt concentration of 35 g L^{-1} . Despite the comparably lower concentration gradient at longer HRT (32.3 mS cm^{-1} at 1.7 d compared with 39.6 mS cm^{-1} at 1.0 d) (Fig. 4B), the effect of molecule transport was greater (2.52% at 1.7 d compared with 1.71% at 1.0 d). The higher ratio between the osmotic water flux and salt solution flow rate (0.14 at 1.7 d HRT, higher than 0.10 at 1.0 d HRT) explained the elevated molecule transport (Fig. 4C). With high current generation, the osmotic water flux that led to molecule transport played an important role in back diffusion.

Those results suggest that back diffusion of inorganic ions under electricity generation could be minor. A longer salt retention time does not lead to more back diffusion as a consequence of the smaller concentration gradient as well as the resulted lower osmotic water flux, especially for desalinating brackish water.²⁴ However, using MDCs as a pretreatment desalination process of seawater is more likely to cause more back diffusion contamination due to a higher concentration gradient (higher osmotic water flux) between the anolyte and salt solution. The ratio between osmotic water flux and salt solution flow rate needs to be precisely designed in real application to minimize back diffusion.

3.3. Organic back diffusion

Three organics were tested in the anode of MDC, NaAc, paracetamol and ibuprofen with molecular weight of 82, 151, and 206 Da, respectively. The open circuit test showed back diffusion percentage of $16 \pm 0.5\%$, $1.3 \pm 0.8\%$, and $2.8 \pm 1.1\%$ for acetate, PCM, and IBP, respectively. Applying an external resistor of 10Ω with a current generation of $1.2 \pm 0.5 \text{ A m}^{-3}$ reduced the back diffusion of acetate and IBP slightly to $12.1 \pm 3.2\%$ and $2.1 \pm 1.5\%$, whereas no reduction was observed with PCM ($2.9 \pm 1.7\%$) due to its neutral charge and negligible biological degradation in the presence of acetate (more readily degradable) (Fig. 5A). High back diffusion of acetate in this batch mode MDC was due to the limitation of low bacteria consumption rate/low current generation that led to a high acetate concentration gradient between the anolyte and desalinated stream throughout the test period in both OC and current modes. The high acetate concentration left in the anolyte (1600 mg L^{-1} with OC and 1300 mg L^{-1} with current at the end of the 48-h batch test) and the salt concentration gradient (10 g L^{-1} at 0-h and $6 \pm 1 \text{ g L}^{-1}$ at 48-h) that would lead to a considerable amount of osmotic water flux likely determined that the dominant mechanism of acetate back diffusion was molecule transport, and current generation (reduced Donnan effect) had relatively less impact on back diffusion. Back diffusion of PCM and IBP was very low, probably because of their higher molecular size.

To eliminate the factor of bacterial degradation of organics, experiments were carried out in an abiotic MDC to examine the effect of salt concentration in desalination compartment on back

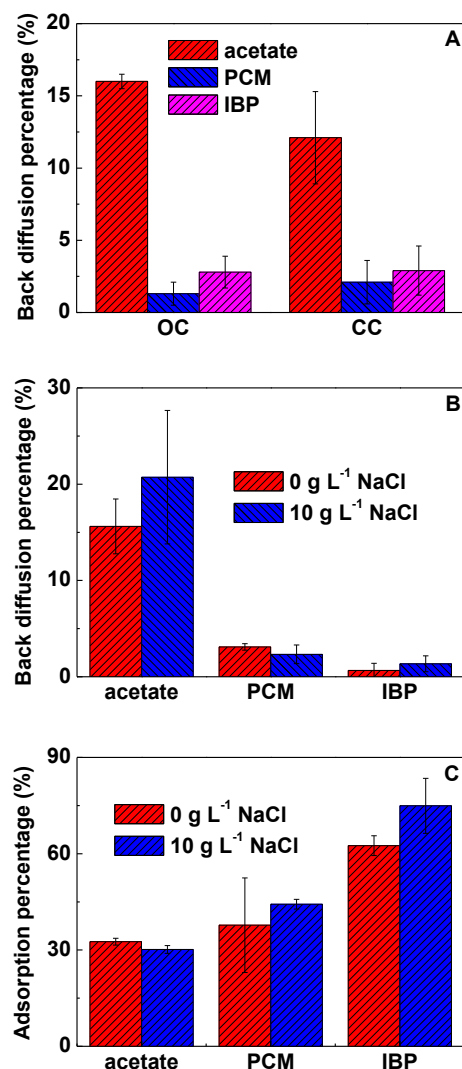


Fig. 5. Back diffusion of selected organic compounds: (A) back diffusion in an MDC under open and closed circuit conditions; (B) back diffusion in an abiotic MDC with 0 g L^{-1} and 10 g L^{-1} NaCl in the desalination compartment; and (C) adsorption of three organic compounds on the AEM in abiotic MDC with 0 g L^{-1} and 10 g L^{-1} NaCl in the desalination compartment.

diffusion of three representative organics with the same initial concentration 100 mg L^{-1} . Results were compared under two conditions, with 0 or 10 g L^{-1} NaCl solution in the desalination compartment, which resulted in $15.6 \pm 2.8\%$ or $20.7 \pm 6.9\%$ back diffusion of acetate, $3.1 \pm 0.3\%$ or $2.3 \pm 1.0\%$ back diffusion of PCM, $0.7 \pm 0.7\%$ or $1.3 \pm 0.8\%$ back diffusion of IBP (Fig. 5B). Control experiments conducted with equal concentrations of organics in both anode and desalination compartment (no organic concentration gradient or salt concentration gradient) showed no back diffusion. With 0 g L^{-1} NaCl in the desalination compartment, no salt concentration gradient was present between the anode and desalination compartments, and molecule transport due to organic concentration gradient was the sole driving force for back diffusion. Acetate was most prone to back diffusion followed by PCM and IBP, and the trend is relevant to their molecular weight ($\text{NaAc} < \text{PCM} < \text{IBP}$) that leads to diffusion coefficient ($\text{NaAc} > \text{PCM} > \text{IBP}$), which is in accordance with Fick's law stating that under the same concentration gradient, the molecules with the larger diffusion coefficient will have greater flux. Under the influence of additional 10 g L^{-1} salt concentration in the desalination

compartment, both Donnan effect and intensified molecule transport (due to osmotic water flux of 9 ± 3 mL from the anolyte to the salt solution) enhanced the back diffusion of acetate, while the effect on IBP and PCM was not notable. It is worth noting that PCM was only subjected to molecule transport because of its neutral charge. The large molecular weight and hydrophobicity of PCM and IBP possibly hindered their crossing over the AEM, leaving them trapped in the hydrophobic AEM (contact angle of 87.0 ± 3.5). The adsorption of organics on the AEM was $32.6 \pm 1.1\%$ under salt effect ($30.2 \pm 1.2\%$ under no salt effect) for acetate, $37.7 \pm 14.7\%$ ($44.3 \pm 1.5\%$) for PCM and $62.5 \pm 3.1\%$ ($74.9 \pm 8.6\%$) for IBP (Fig. 5C). The larger amount of organics trapped in the AEM with additional salt present in the desalination compartment clearly demonstrates the more intense movement of organics towards the desalination compartment under effect of osmotic water flux (and Donnan effect for charged organics). The absorption intensity order was $IBP > PCM > NaAc$, which is closely correlated to their molecular weight and hydrophobicity ($IBP > PCM > NaAc$). The larger molecular weight and greater hydrophobicity, the more likely the compound would be trapped by the AEM, and not cause back diffusion in the salt solution.

3.4. Principal component analysis

To further analyze the key factors affecting back diffusion (continuous mode), variables such as current, concentration difference between the salt solution and the anolyte, osmotic water flux, as well as the ratio between osmosis flux and salt flow rate were taken into account and processed through principal component analysis (PCA). The PCA biplot mainly separated the MDC performance into two major groups associated with different initial salt concentrations of 5 g L^{-1} and 35 g L^{-1} , with Principal Component 1 (PC1) and Principal Component 2 (PC2) picking up 52.1% and 37.4% of the variation of the data, respectively, and 89.5% in total (Fig. 6). A close positive correlation between concentration gradient related variables and molecule transport was shown, as well as a negative correlation between current and Donnan effect, supporting our conclusion that a higher concentration gradient promotes molecule transport, and higher current inhibits Donnan effect. The scree plot with parallel analysis shows the eigenvalues of two components are above 1 suggesting that appropriate number of principal components is two, and thus a rotation method “varimax” with two components were performed in order to clarify the structure of the loadings matrix. The off diagonal fitting was achieved at 99%. The first rotated component heavily loaded on molecule transport, the concentration gradient, osmotic water flux, as well as the ratio between osmosis flux and salt flow rate (0.81–0.97), which further confirmed the close association between the four variables, indicating that molecule transport back diffusion increases with a higher concentration gradient/osmotic water flux. The second rotated component is strongly associated with Donnan effect (0.96), and negatively loaded on current (-0.92), which suggests the negative correlation between the two variables and that Donnan effect decreases with stronger current. The variable back diffusion of anions was heavily loaded on the second rotated component (0.93), which explains the effect of current was more potent than concentration gradient on back diffusion (Table 1). It can be concluded that with high current generation, concentration gradient will be diminished and thus molecule transport can be minimized.

4. Conclusions

This study has presented two mechanisms for contaminant back diffusion from the anolyte into the desalinated stream in an MDC,

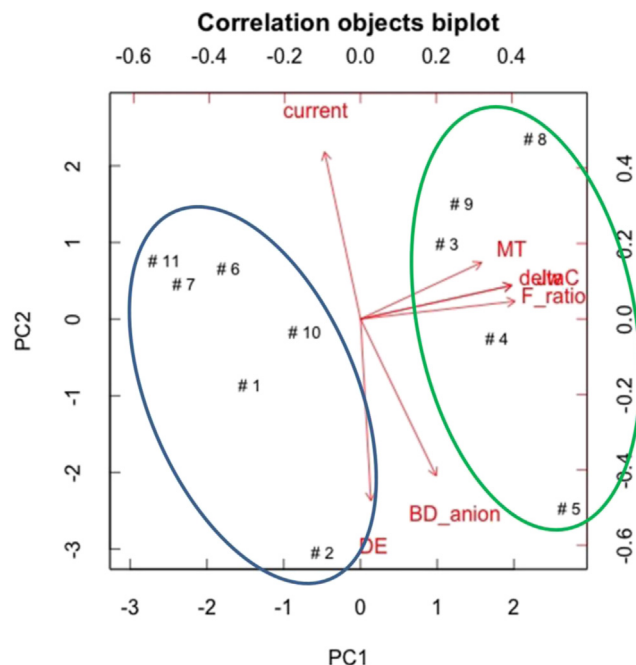


Fig. 6. PCA biplot with scores and loadings for MDC plotted on the first two components, where the number labeled points are the MDC with different operation conditions (in terms of initial salt concentration and external resistance), MT is the molecule transport, DE is the Donnan effect, BD_anion is the back diffusion of anions, deltaC is the concentration difference between the anolyte and the salt solution, Jw is the osmotic water flux, and F_ratio is the ratio of osmotic water flux over salt flow rate.

Table 1
Standardized loadings based upon correlation matrix (Principal Components Method with rotation).

	RC1	RC2	h2	u2
Jw	0.97	0.05	0.94	0.057
F_ratio	0.97	0.14	0.96	0.037
deltaC	0.97	0.05	0.94	0.057
current	-0.01	-0.92	0.85	0.150
BD_anion	0.27	0.93	0.93	0.067
MT	0.81	-0.11	0.68	0.323
DE	-0.16	0.96	0.95	0.049

Donnan effect for negatively charged ion exchange and molecule transport driven by osmotic water flux. Current generation could inhibit Donnan effect and result in relatively higher percentage of molecule transport. Organic matters with a larger molecular weight and greater hydrophobicity could be retained by the AEM resulting in less back diffusion. Desalinating a higher-salinity stream (e.g., seawater) will likely cause more back diffusion than that with a low-salinity stream (e.g., brackish water), because of a higher osmotic water flux resulted from a greater concentration gradient between the anolyte and salt solution. The ratio between osmotic water flux and salt solution flow rate was found to be a critical design criterion for MDC development. These findings have enhanced our understanding of back diffusion in MDCs and provide useful information for the further development.

Acknowledgments

This project was financially supported by Research Grant Award No. US-4455-11 from BARD, the United States–Israel Binational Agricultural Research and Development Fund.

Appendix A. Supplementary data

Supplementary data related to this article can be found at <http://dx.doi.org/10.1016/j.watres.2015.10.018>.

References

- Cao, X.X., Huang, X., Liang, P., Xiao, K., Zhou, Y.J., Zhang, X.Y., Logan, B.E., 2009. A new method for water desalination using microbial desalination cells. *Environ. Sci. Technol.* 43 (18), 7148–7152.
- Chen, X., Xia, X., Liang, P., Cao, X.X., Sun, H.T., Huang, X., 2011. Stacked microbial desalination cells to enhance water desalination efficiency. *Environ. Sci. Technol.* 45 (6), 2465–2470.
- Chen, S., Liu, G., Zhang, R., Qin, B., Luo, Y., 2012b. Development of the microbial electrolysis desalination and chemical-production cell for desalination as well as acid and alkali productions. *Environ. Sci. Technol.* 46 (4), 2467–2472.
- Chen, X., Liang, P., Wei, Z., Zhang, X., Huang, X., 2012a. Sustainable water desalination and electricity generation in a separator coupled stacked microbial desalination cell with buffer free electrolyte circulation. *Bioresour. Technol.* 119, 88–93.
- Forrestal, C., Xu, P., Jenkins, P.E., Ren, Z.Y., 2012. Microbial desalination cell with capacitive adsorption for ion migration control. *Bioresour. Technol.* 120, 332–336.
- Ge, Z., Dosoretz, C.G., He, Z., 2014. Effects of number of cell pairs on the performance of microbial desalination cells. *Desalination* 341, 101–106.
- Gur-Reznik, S., Azerrad, S.P., Levinson, Y., Heller-Grossman, L., Dosoretz, C.G., 2011. Iodinated contrast media oxidation by nonthermal plasma: the role of iodine as a tracer. *Water Res.* 45 (16), 5047–5057.
- Jacobson, K.S., Drew, D.M., He, Z., 2011a. Use of a liter-scale microbial desalination cell as a platform to study bioelectrochemical desalination with salt solution or artificial seawater. *Environ. Sci. Technol.* 45 (10), 4652–4657.
- Jacobson, K., Drew, D., He, Z., 2011b. Efficient salt removal in a continuously operated upflow microbial desalination cell with an air cathode. *Bioresour. Technol.* 102 (1), 376–380.
- Kim, Y., Logan, B., 2011. Series assembly of microbial desalination cells containing stacked electro dialysis cells for partial or complete seawater desalination. *Environ. Sci. Technol.* 45 (13), 5840–5845.
- Kim, Y., Logan, B.E., 2013. Microbial desalination cells for energy production and desalination. *Desalination* 308, 122–130.
- Luo, H., Jenkins, P., Ren, Z., 2011. Concurrent desalination and hydrogen generation using microbial electrolysis and desalination cells. *Environ. Sci. Technol.* 45 (1), 340–344.
- Luo, H.P., Xu, P., Jenkins, P.E., Ren, Z.Y., 2012a. Ionic composition and transport mechanisms in microbial desalination cells. *J. Membr. Sci.* 409, 16–23.
- Luo, H.P., Xu, P., Roane, T.M., Jenkins, P.E., Ren, Z.Y., 2012b. Microbial desalination cells for improved performance in wastewater treatment, electricity production, and desalination. *Bioresour. Technol.* 105, 60–66.
- Mehanna, M., Saito, T., Yan, J., Hickner, M., Cao, X., Huang, X., Logan, B., 2010. Using microbial desalination cells to reduce water salinity prior to reverse osmosis. *Energy Environ. Sci.* 3 (8), 1114–1120.
- Ping, Q.Y., He, Z., 2013. Improving the flexibility of microbial desalination cells through spatially decoupling anode and cathode. *Bioresour. Technol.* 144, 304–310.
- Ping, Q.Y., Cohen, B., Dosoretz, C., He, Z., 2013. Long-term investigation of fouling of cation and anion exchange membranes in microbial desalination cells. *Desalination* 325, 48–55.
- Ping, Q.Y., He, Z., 2014. Effects of inter-membrane distance and hydraulic retention time on the desalination performance of microbial desalination cells. *Desalin. Water Treat.* 52 (7–9), 1324–1331.
- Ping, Q.Y., Zhang, C.Y., Chen, X.E., Zhang, B., Huang, Z.Y., He, Z., 2014. Mathematical model of dynamic behavior of microbial desalination cells for simultaneous wastewater treatment and water desalination. *Environ. Sci. Technol.* 48 (21), 13010–13019.
- Ping, Q.Y., Huang, Z.Y., Dosoretz, C., He, Z., 2015. Integrated experimental investigation and mathematical modeling of brackish water desalination and wastewater treatment in microbial desalination cells. *Water Res.* 77, 13–23.
- Qu, Y.P., Feng, Y.J., Wang, X., Liu, J., Lv, J.W., He, W.H., Logan, B.E., 2012. Simultaneous water desalination and electricity generation in a microbial desalination cell with electrolyte recirculation for pH control. *Bioresour. Technol.* 106, 89–94.
- Strathmann, H., 2004. Ion-exchange Membrane Separation Processes. Elsevier B.V. Amsterdam.
- Vanderford, B.J., Pearson, R.A., Rexing, D.J., Snyder, S.A., 2003. Analysis of endocrine disruptors, pharmaceuticals, and personal care products in water using liquid chromatography/tandem mass spectrometry. *Anal. Chem.* 75 (22), 6265–6274.
- Velasquez-Orta, S.B., Head, I.M., Curtis, T.P., Scott, K., Lloyd, J.R., von Canstein, H., 2010. The effect of flavin electron shuttles in microbial fuel cells current production. *Appl. Microbiol. Biotechnol.* 85 (5), 1373–1381.
- Yuan, H.Y., Abu-Reesh, I.M., He, Z., 2015. Enhancing desalination and wastewater treatment by coupling microbial desalination cells with forward osmosis. *Chem. Eng. J.* 270, 437–443.
- Zhang, B., He, Z., 2012. Integrated salinity reduction and water recovery in an osmotic microbial desalination cell. *Rsc Adv.* 2 (8), 3265–3269.
- Zhang, F., Chen, M., Zhang, Y., Zeng, R., 2012. Microbial desalination cells with ion exchange resin packed to enhance desalination at low salt concentration. *J. Membr. Sci.* 417, 28–33.
- Zhang, F., He, Z., 2015. Scaling up microbial desalination cell system with a post-aerobic process for simultaneous wastewater treatment and seawater desalination. *Desalination* 360, 28–34.
- Zuo, K.C., Yuan, L.L., Wei, J.C., Liang, P., Huang, X., 2013. Competitive migration behaviors of multiple ions and their impacts on ion-exchange resin packed microbial desalination cell. *Bioresour. Technol.* 146, 637–642.